NACA

RESEARCH MEMORANDUM

for the

U. S. Air Force

DRAG MEASUREMENTS AT ZERO LIFT ON A 1/10-SCALE MODEL OF THE MX-1626 SUPERSONIC BOMBER AT TRANSONIC SPEEDS

By John M. Swihart and Robert L. O'Neal

Langley Aeronautical Laboratory
Langley Field, Va.

NATIONAL ADVISORY COMMITTEE
FOR AERONAUTICS
WASHINGTON

NACA RM SL53D27a

NATIONAL ADVISORY COMMITTEE FOR AERONAUTICS

RESEARCH MEMORANDUM

for the

U. S. Air Force

DRAG MEASUREMENTS AT ZERO LIFT ON A 1/10-SCALE MODEL OF THE MX-1626 SUPERSONIC BOMBER AT TRANSONIC SPEEDS

By John M. Swihart and Robert L. O'Neal

SUMMARY

An investigation to determine the zero-lift drag of a 1/10-scale model of the MX-1626 supersonic bomber has been conducted in the Langley 16-foot transonic tunnel. The Mach number range was from 0.80 to 1.09 and the Reynolds number range was from 13.0×10^6 to 13.3×10^6 based on a mean aerodynamic chord of 3.38 feet.

The results of the investigation indicate that the maximum drag coefficient for the complete model with closed nacelles was 0.036 at a Mach number of 1.04 and that there is generally good agreement between the free-flight data and the adjusted wind-tunnel data. The drag coefficient for the model with open nacelles was 0.032 at a Mach number of 1.04 and was reduced to 0.027 when the landing-gear fairings were removed. There was no reduction in maximum drag coefficient when the two upper parts of the triadic-pod tail were removed.

INTRODUCTION

Flight tests of a rocket-powered model of the MX-1626 supersonic bomber conducted by the Langley Pilotless Aircraft Research Division indicated values of drag coefficient higher than had been anticipated in the bomber's design. Because the anticipated drag estimates were based on supersonic wind-tunnel tests of very small-scale models where the rear end of the models had been enlarged to accommodate a sting of sufficient size to carry loads at high angles of attack, an independent

test of a model identical to the rocket-powered model was made in the Langley 16-foot transonic tunnel.

This paper presents the results of drag measurements at zero lift made with a 1/10-scale model of the MX-1626 supersonic bomber in the Langley 16-foot transonic tunnel. Several additional tests were made to investigate the effect on drag of air flow through the nacelles, drag due to landing-gear fairings, and the triadic fins on the pod.

Zero lift was maintained on the model and the drag was measured over a Mach number range from 0.80 to 1.09. The average Reynolds number based on a mean aerodynamic chord of 3.38 feet varied from 13.0×10^6 to 13.3×10^6 in the Mach number range from 0.80 to 1.09.

APPARATUS

Langley 16-Foot Transonic Tunnel

This investigation was conducted in the slotted test section of the Langley 16-foot transonic tunnel. A complete description and calibration of this tunnel is given in reference 1 and figure 1 shows the model installed in the test section.

Model

A 1/10-scale model of the MX-1626 supersonic bomber was used for this investigation. The model is constructed of magnesium and mahogany and is identical to the rocket-powered model tested by the Langley Pilotless Aircraft Research Division. A sketch of the model and sting assembly is shown in figure 2 and dimensions for the model are given in table I. The wing is of delta plan form with the leading edge swept back 65° and NACA 65A004 airfoil sections parallel to the plane of symmetry. The pod and fuselage are designed to separate on the parting line shown in figure 2. The nacelles are set at a negative angle of incidence of 2.13° with respect to the wing.

Two nacelle configurations, closed and open, were used in this investigation and the closed configuration was obtained by fairing the nose and sealing the base of the nacelle. The closed nacelle configuration is shown in figure 3(a) with a plug located in the exit of each nacelle flush with the nacelle base. Figure 3(b) shows the open nacelle configuration with the central spike at the inlet and the plugs removed from the nacelle exit. Table II gives the dimensions of both nacelle configurations and the nacelle central spike.

Figure 4 shows the landing-gear fairings installed on the model. The landing-gear fairings and the two upper parts of the triadic-pod tail shown in figure 2 were removed for a part of the investigation. The model was maintained in a clean and fair condition during the investigation.

Support Strut and Sting Assembly

Figure 1(b) shows the support configuration used for this investigation. The main support is a vertical cantilever strut of circular-arc cross section capped with a 14-inch-diameter cylindrical body and the cone-shaped sting is faired into this cylinder.

The sting was cylindrical for 6 inches behind the model base in order to keep sting interference as low as possible. Two wooden cuffs were installed over the sting to move the sting cone in relation to the model base to study the effect of sting-cone interference. Figure 2 shows the wooden cuffs and their position relative to the model base.

TESTS AND MEASUREMENTS

Test Conditions

The drag of the model was measured over a Mach number range from 0.80 to 1.09 with the model lift maintained at or near zero by small ($\pm 0.2^{\circ}$) adjustments in angle of attack. The average Reynolds number based on a mean aerodynamic chord of 3.38 feet was from 13.0×10^6 to 13.3×10^6 in the Mach number range from 0.80 to 1.09.

Instrumentation and Measurements

The aerodynamic forces on the model were measured by a 6-component strain-gage balance. The balance was mounted on the sting which entered the stern of the pod, and the model was bolted through the wing directly to the balance. The drag component capacity of the only balance available for this work was much greater than would normally have been selected; therefore, the results suffer in accuracy and data are not presented at speeds below a Mach number of 0.80. The drag-coefficient and pitching-moment-coefficient measurements can be repeated to ± 0.001 at a Mach number of 1.0, and the error is inversely proportional to dynamic pressure. The Mach numbers quoted in this paper are accurate to ± 0.01.

[redacted]

Four pressure orifices were located 1/2 inch inside the pod base to measure the pod base pressure. Two pressure orifices were located in the nacelle base plug to measure the nacelle base pressure during the closed-nacelle investigation. Figure 5 shows the variation of nacelle and pod base-pressure coefficient with Mach number. The data for the closed-nacelle configuration have been adjusted to the condition of nacelle base pressure and pod base pressure equivalent to free-stream static pressure. All open-nacelle-configuration data have also been adjusted to the condition of pod base pressure equivalent to free-stream static pressure.

Figure 3(b) shows the location of the total head rake and static-pressure orifices inside the nacelle exit. These pressures were measured to determine the internal drag of the open nacelles. Figure 6 shows the variation of internal drag coefficient of the open nacelles with Mach number. The curve represents the average of five runs with open nacelles and no point is more than 0.0001 from the faired line with a great many points being coincident. The internal drag was computed by the method of reference 2 where internal drag is defined as

$$D_i = m\left(V_o - V_{exit}\right) + A_{exit}\left(p_o - p_{exit}\right)$$

where m is the mass flow; V, the velocity; A, the area; p, the static pressure; and the subscripts o and $exit$ denote free-stream and nacelle-exit conditions. This quantity with a reversal of sign is the usual expression for turbojet engine thrust. The internal drag of the open nacelles has been subtracted from the measured drag for all open nacelle data presented in this paper.

RESULTS AND DISCUSSION

Comparison of Langley 16-Foot Transonic Tunnel Data With Free-Flight Results

Figure 7 presents the variation of drag coefficient with Mach number for the rocket-powered flight model of the Langley Pilotless Aircraft Research Division (unpublished) and for an identical model investigated in the Langley 16-foot transonic tunnel. The nacelles were closed and the landing-gear fairings were attached in both cases. The experimental data of the 16-foot transonic-tunnel show a drag coefficient of about 0.01 in the low-speed range and a rapid rise near a Mach number of 0.925 to a maximum value of 0.036 at a Mach number of 1.04. The drag-coefficient peak near a Mach number of 1.04 followed by the reduction with a further

increase in Mach number is a characteristic trend of drag measurements at low supersonic speeds in wind tunnels where wall-reflected disturbances are present.

Reference 3 presents transonic drag measurements on a 33.33-inch-long body of revolution with a fineness ratio of 10 in the Langley 8-foot transonic tunnel where disturbances originating at the bow are reflected symmetrically from the tunnel walls and converge as a concentrated disturbance on the model. The net effect is to increase the drag at very low supersonic speeds and to decrease the drag at slightly higher speeds. Reference 4 presents the drag data of a 45° sweptback wing-fuselage combination and indicates that wall-reflected disturbances increase the drag coefficient of the wing-fuselage combination by 0.002 at $M = 1.04$ and decrease the drag coefficient by 0.002 at $M = 1.09$. At speeds where the reflected disturbances no longer intersect the model, the drag will be unaffected. It is believed that similar disturbances exist in the Langley 16-foot transonic tunnel at these supersonic speeds which would cause the reduction in the experimental drag-coefficient points obtained for this model in the Mach number range from 1.04 to 1.08. Figure 7 shows an estimated adjustment to the drag coefficient for the complete model in the low-supersonic speed range. This adjustment is based on information obtained from investigations in the 16-foot and 8-foot transonic tunnels where wall-reflected disturbances were noted. It is believed that this adjustment to the wind-tunnel data represents the drag data that would be obtained in an interference-free condition. There is generally good agreement between the free-flight data and the adjusted wind-tunnel data.

Effect on Drag Coefficient of Open Nacelles, Landing-Gear Fairings, and Triadic-Pod Tail

Figure 8 presents a comparison of the variation in drag coefficient with Mach number for four different model configurations. The drag coefficient was reduced at the maximum value from 0.036 to 0.032 at a Mach number of 1.04 when the closed nacelles were replaced by open nacelles. It is believed that the negative pressures existing at the base of the closed nacelles influenced the surface pressures over the rearward portions of the nacelles and the wing. Air flow through the nacelles eliminates this negative pressure field and a lower drag coefficient is realized. The mass-flow ratio was 0.94 and indicates that there was no excessive external drag due to spillage over the nacelle.

The landing-gear fairings were removed from the open-nacelle model in order to investigate the effect of these protuberances on the drag of the model. The fairings are almost rectangular in cross section but

are airfoil-shaped in plan form. At the point of maximum thickness, the landing-gear fairings are in contact with the pod. It was believed that the landing-gear fairing-pod juncture would cause a high interference drag and that a sharp drag reduction would result if the fairings were removed. A slight drag reduction might be expected because some frontal area is being removed and the area distribution would be improved (see ref. 5). Figure 8 shows that there is a general reduction in drag coefficient for the Mach number range from 0.80 to 1.09 when the landing-gear fairings were removed from the open-nacelle configuration and, at $M = 1.04$, there is a decrease in drag coefficient from 0.032 to 0.027, which is a reduction of approximately 15 percent.

Shadowgraphs taken during the investigation indicated some shock interferences in the region of the vertical tail, the two upper parts of the triadic-pod tail, and the wing trailing edge. In order to determine the magnitude of the drag associated with these shocks, the two upper parts of the triadic-pod tail were removed. Figure 8 shows that there is no reduction in drag coefficient greater than the experimental accuracy when the two upper parts of the triadic-pod tail are removed from the configuration with open nacelles and landing-gear fairings removed.

Pitching-Moment Coefficient

The zero-lift pitching moment was measured for all configurations over the Mach number range. The wing-fuselage pitching-moment coefficient about the one-fourth mean aerodynamic chord is essentially zero in the Mach number range from 0.80 to 1.09.

Effect of Sting Cone and Sting on Drag Coefficient

In order to evaluate the interference forces caused by the presence of the sting cone, two wooden cuffs were added to the sting which effectively moved the 5° sting-cone angle to the model base. It would be expected that the positive pressure field of the cone would act on the rearward portions of the model and cause a reduction in drag. Figure 9 shows the effect of adding sting cuffs on the drag coefficient of the complete model with open nacelles. Inasmuch as the addition of two cuffs and one cuff showed no appreciable effect, it is believed that the no-cuff condition used for this investigation is effectively free of interference from the sting cone. Reference 6 shows the effect on model drag coefficient of various ratios of sting diameter to base diameter. These effects of the sting on the model drag have not been adjusted for the condition of base pressure equivalent to free-stream static pressure and include, therefore, the effects of the sting on the base pressure.

Consideration of the magnitude of the sting interference of reference 6 and the fact that the base pressure has been adjusted to free-stream static pressure for these tests as well as the fact that the ratio of wing area to model base area for this model is only one-fourth as much as that for the more conventional wind-tunnel model of reference 6 leads to the belief that the effect of sting interference is small for these tests.

CONCLUSIONS

An investigation to determine the zero-lift drag of a 1/10-scale model of the MX-1626 supersonic bomber over a Mach number range from 0.80 to 1.09 has led to the following conclusions:

1. The low-speed drag coefficient is about 0.01 and the maximum drag coefficient is 0.036 at a Mach number of 1.04 for the complete model with closed nacelles. There is generally good agreement between the free-flight data and the adjusted wind-tunnel data.

2. Air flow through the open nacelles at a mass-flow ratio of 0.94 reduced the maximum drag coefficient to 0.032 at a Mach number of 1.04.

3. The drag coefficient of the model with open nacelles was reduced 0.005 at a Mach number of 1.04 when the landing-gear fairings were removed.

4. There was no measurable reduction in drag coefficient when the two upper parts of the triadic-pod tail were removed.

Langley Aeronautical Laboratory,
National Advisory Committee for Aeronautics,
Langley Field, Va.

John M. Swihart
John M. Swihart
Aeronautical Research Scientist

Robert L. O'Neal
Robert L. O'Neal
Aeronautical Research Scientist

Approved:
Eugene C. Draley
Eugene C. Draley
Chief of Full Scale Research Division

vr

[redacted]

REFERENCES

1. Ward, Vernon G., Whitcomb, Charles F., and Pearson, Merwin D.: Air-Flow and Power Characteristics of the Langley 16-Foot Transonic Tunnel With Slotted Test Section. NACA RM L52E01, 1952.

2. Pendley, Robert E., Milillo, Joseph R., and Fleming, Frank F.: An Investigation of Three NACA 1-Series Nose Inlets at Subsonic and Transonic Speeds. NACA RM L52J23, 1953.

3. Ritchie, Virgil S., and Pearson, Albin O.: Calibration of the Slotted Test Section of the Langley 8-Foot Transonic Tunnel and Preliminary Experimental Investigation of Boundary-Reflected Disturbances. NACA RM L51K14, 1952.

4. Osborne, Robert S., and Mugler, John P., Jr.: Aerodynamic Characteristics of a 45° Sweptback Wing-Fuselage Combination and the Fuselage Alone Obtained in the Langley 8-Foot Transonic Tunnel. NACA RM L52E14, 1952.

5. Whitcomb, Richard T.: A Study of the Zero-Lift Drag-Rise Characteristics of Wing-Body Combinations Near the Speed of Sound. NACA RM L52H08, 1952.

6. Osborne, Robert S.: High-Speed Wind-Tunnel Investigation of the Longitudinal Stability and Control Characteristics of a $\frac{1}{16}$-Scale Model of the D-558-2 Research Airplane at High Subsonic Mach Numbers and at a Mach Number of 1.2. NACA RM L9C04, 1949.

[redacted]

TABLE I.- DIMENSIONS OF THE 1/10-SCALE MODEL OF THE MX-1626 SUPERSONIC BOMBER

Wing:		
Area, sq in.		1728
Span, in.		56.721
Root chord, in.		60.874
Length of M.A.C., in.		40.583
Airfoil section (parallel to plane of symmetry)		NACA 65A004
Sweepback leading edge		65°
Dihedral		-2° 27'
Incidence		0°
Aspect ratio		1.86
Fuselage:		
Over-all length, in.		80.00
Distance from nose of fuselage to leading edge of wing root chord, in.		12.825
Maximum width, in.		5.980
Pod:		
Over-all length, in.		90.162
Distance from pod nose to leading edge of wing root chord, in.		21.025
Maximum width, in.		6.000
Nacelles:	Closed	Open
Over-all length, in.	48.000	42.621
Exit diameter, in.	3.252	3.252
Distance from airplane center line to nacelle center line, in.	16.350	16.350
Vertical tail:		
Total area, sq in.		125.271
Span, in.		13.245
Root chord, in.		18.916
Airfoil section (parallel to root chord)		NACA 65A005
Sweepback leading edge		55°
Pod tails:		
Total area (one fin), sq in.		70.848
Semispan, in.		9.600
Root chord, in.		9.840
Taper ratio		0.500
Airfoil section (parallel to root chord)		NACA 65A005
Sweepback leading edge		52°
Angle between tails		120°

[redacted]

TABLE II.- NACELLE AND NACELLE SPIKE ORDINATES

[See fig. 3]

Nacelle station	Closed nacelle					Open nacelle					
	Radius A	Radius B	Dimension C	Dimension D	Dimension E	Radius A	Radius B	Dimension C	Dimension D	Dimension E	Internal radius
-6.000	0	-----	0	-----	-----	-----	-----	-----	-----	-----	-----
-2.440	.954	-----	1.908	-----	-----	-----	-----	-----	-----	-----	-----
-.621	1.420	-----	2.840	-----	-----	-----	-----	-----	-----	-----	-----
.000	1.545	-----	3.090	-----	-----	-----	-----	-----	-----	-----	-----
.950	1.730	-----	3.460	-----	-----	1.730	0.135	3.460	-----	-----	1.700
2.000	1.895	0.490	3.885	-----	-----	1.895	.505	3.875	-----	-----	1.829
5.000	2.265	1.120	4.890	-----	-----	2.265	1.135	4.870	-----	-----	1.969
8.000	2.485	1.580	5.580	2.485	-----	2.485	1.595	5.555	2.485	-----	2.054
11.000	2.590	1.900	6.000	2.600	-----	2.590	1.915	5.980	2.590	-----	2.113
13.300	2.600	2.050	6.165	2.600	-----	2.600	2.055	6.130	2.600	-----	2.113
16.000	2.600	2.125	6.230	2.600	-----	2.600	2.125	6.230	2.600	-----	2.113
19.000	2.600	2.103	6.200	2.600	2.600	2.600	2.103	6.200	2.600	2.600	2.113
22.000	2.600	2.000	6.100	2.600	2.600	2.600	2.000	6.100	2.600	2.600	2.113
25.000	2.580	1.849	5.913	2.580	2.580	2.580	1.849	5.913	2.580	2.580	2.066
28.000	2.520	1.655	5.640	2.520	2.520	2.520	1.655	5.640	2.520	2.520	1.989
31.000	2.430	1.410	5.273	2.430	2.430	2.430	1.410	5.273	2.430	2.430	1.911
34.000	2.265	1.130	4.815	2.265	2.265	2.265	1.130	4.815	2.265	2.265	1.833
37.000	2.055	.840	4.270	1.965	1.965	2.055	.840	4.270	1.965	1.965	1.756
40.000	1.780	.530	3.628	1.305	1.305	1.780	.530	3.628	1.305	1.305	1.678
42.000	1.562	-----	3.125	.620	.620	1.562	-----	3.125	.620	.620	1.626

Nacelle spike			
Distance G	Ordinate H	Distance K	Ordinate L
0	0	0	0
2.12	.775	1.00	.22
2.62	.890	2.00	.50
3.12	.945	3.00	.69
3.62	.960	4.00	.82
4.12	.950	5.00	.89
4.62	.925	5.40	.90
5.00	.900		

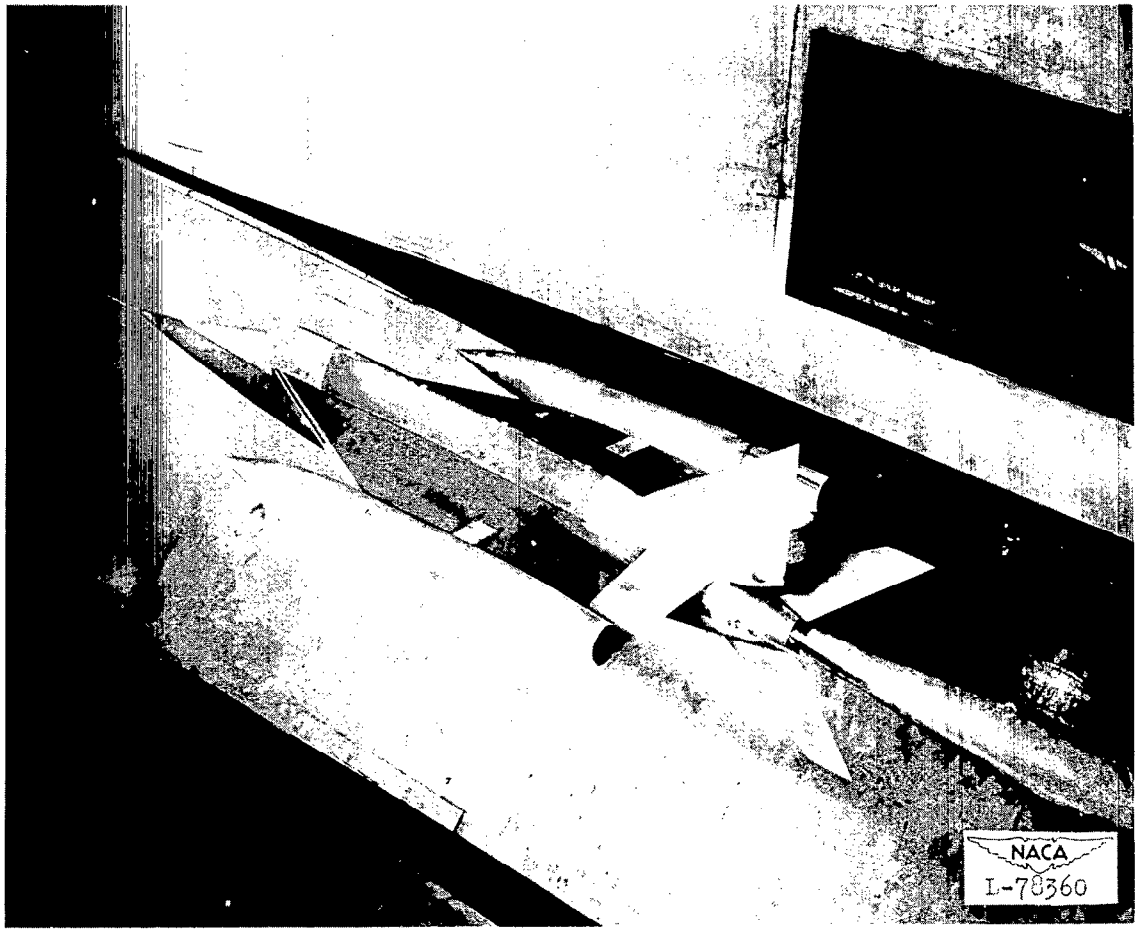

(a) Closed nacelles.

Figure 1.- Three-quarter rear view of the 1/10-scale model of the MX-1626 supersonic bomber installed in the test section of the Langley 16-foot transonic tunnel.

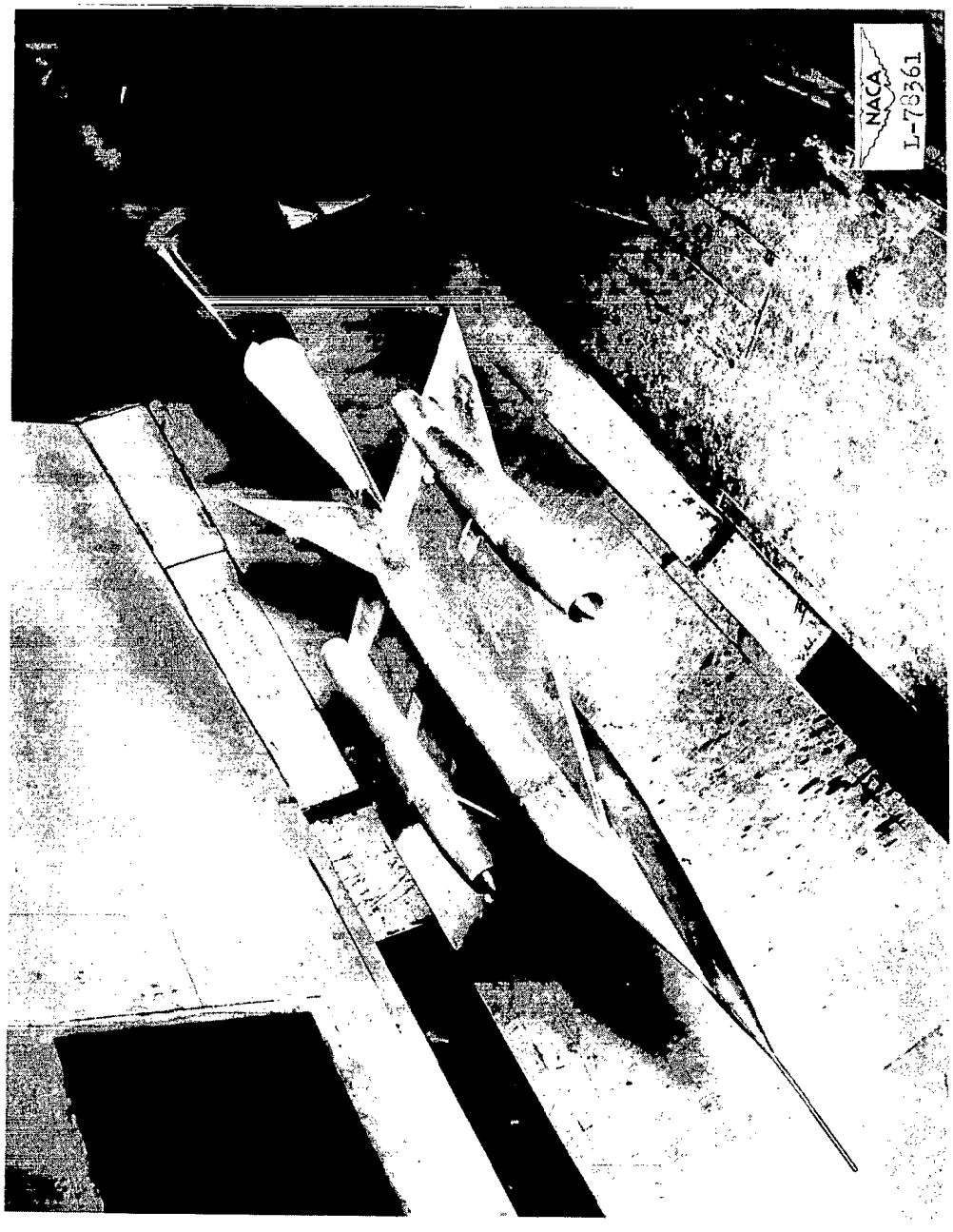

(b) Open nacelles.

Figure 1.- Concluded.

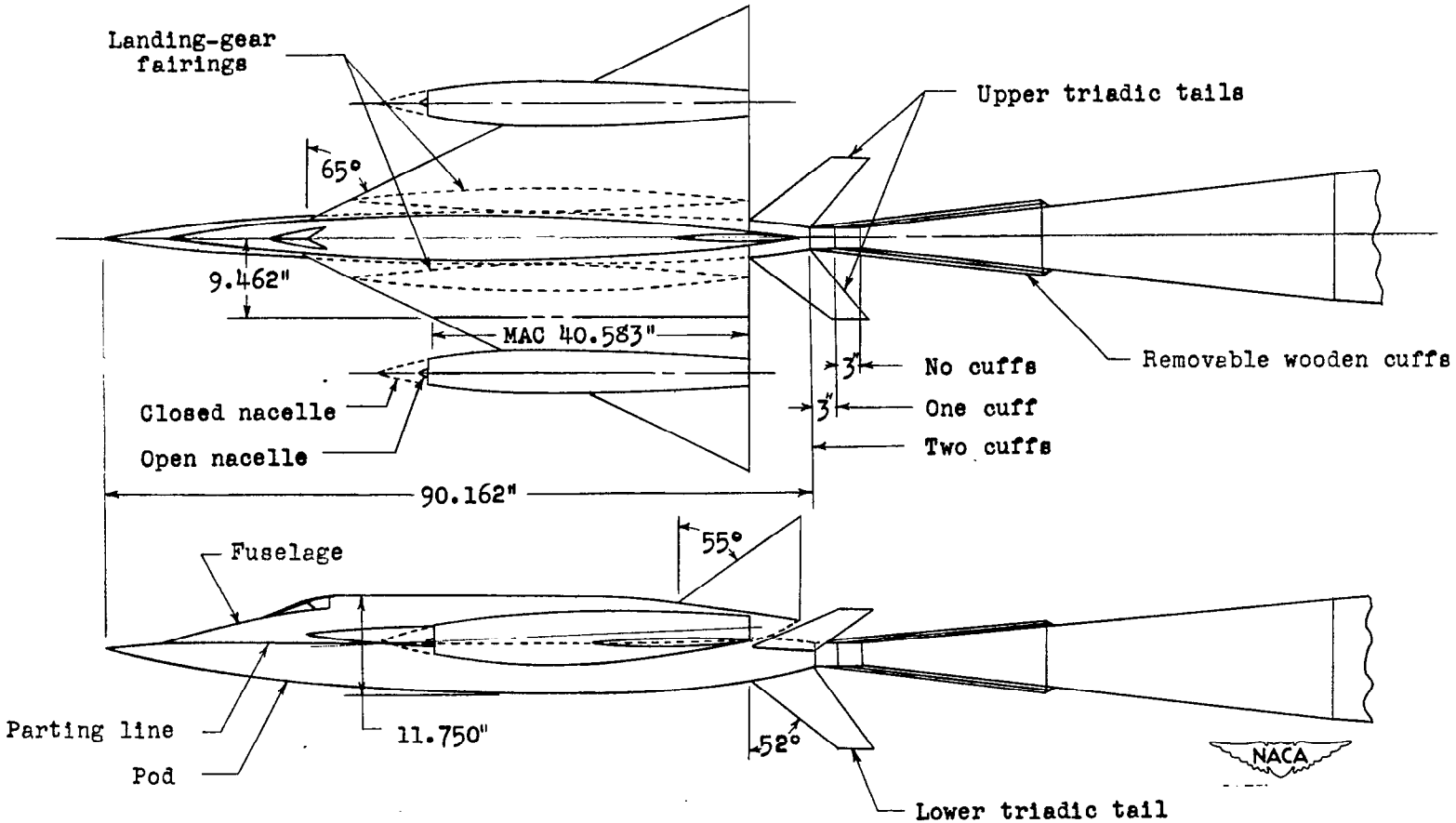

Figure 2.- Sketch of 1/10-scale model of the MX-1626 supersonic bomber and sting assembly.

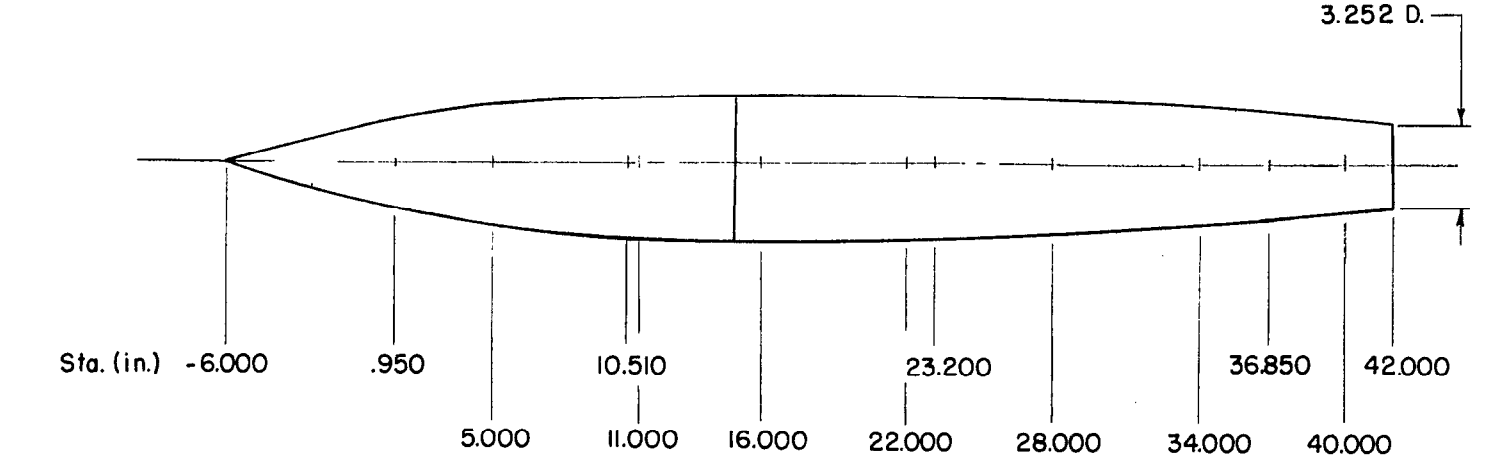

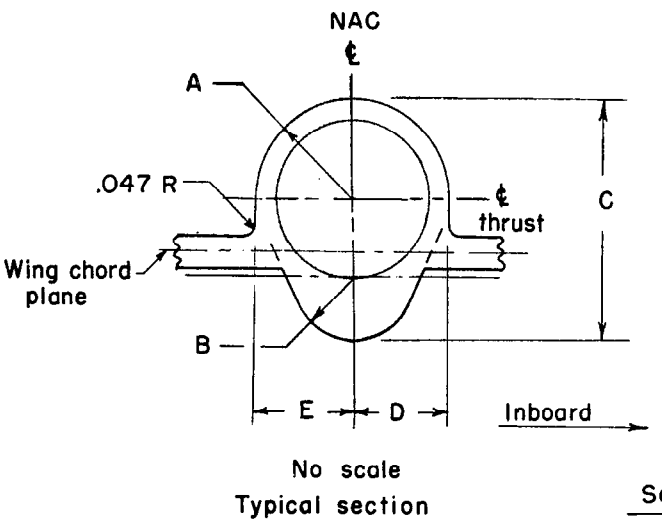

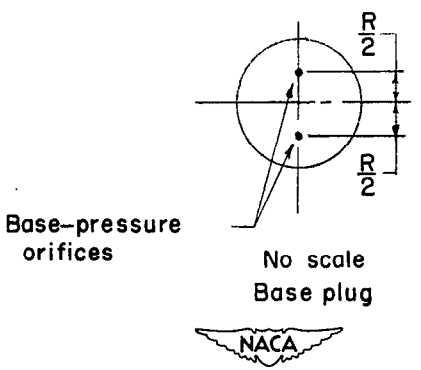

See table II for nacelle dimensions.

(a) Closed nacelle.

Figure 3.- Nacelle configurations.

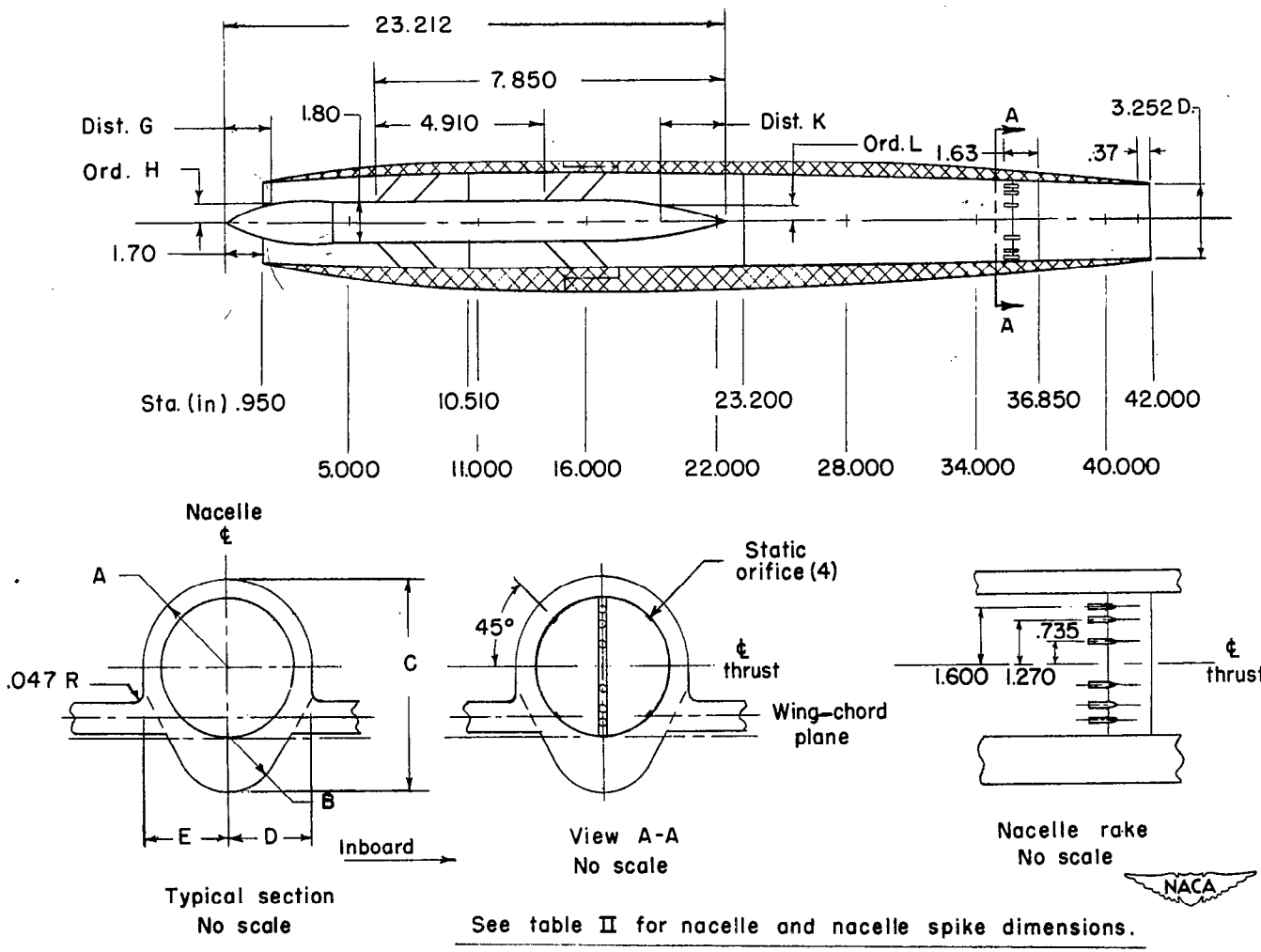

(b) Open nacelle and nacelle spike.

Figure 3.- Concluded.

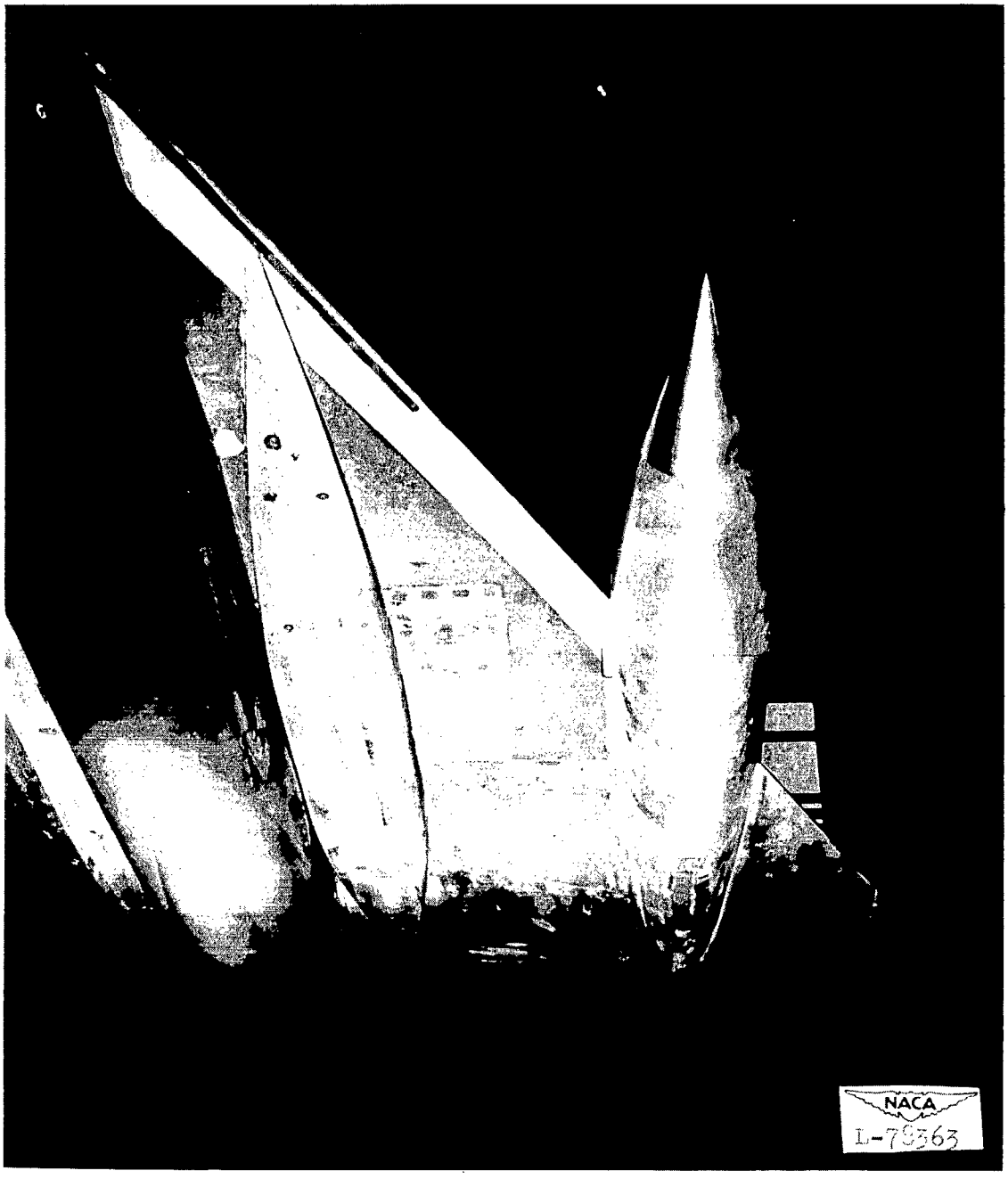

Figure 4.- Landing-gear fairings on the 1/10-scale model of the MX-1626 supersonic bomber.

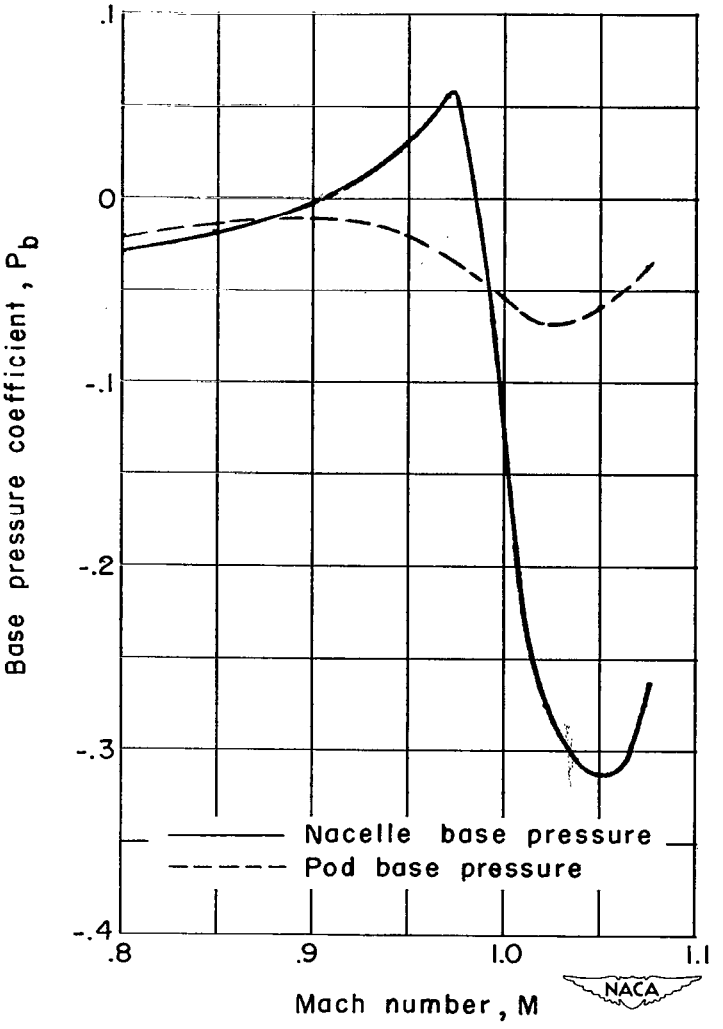

Figure 5.- Variation of nacelle and pod base-pressure coefficient with Mach number for the MX-1626 supersonic bomber.

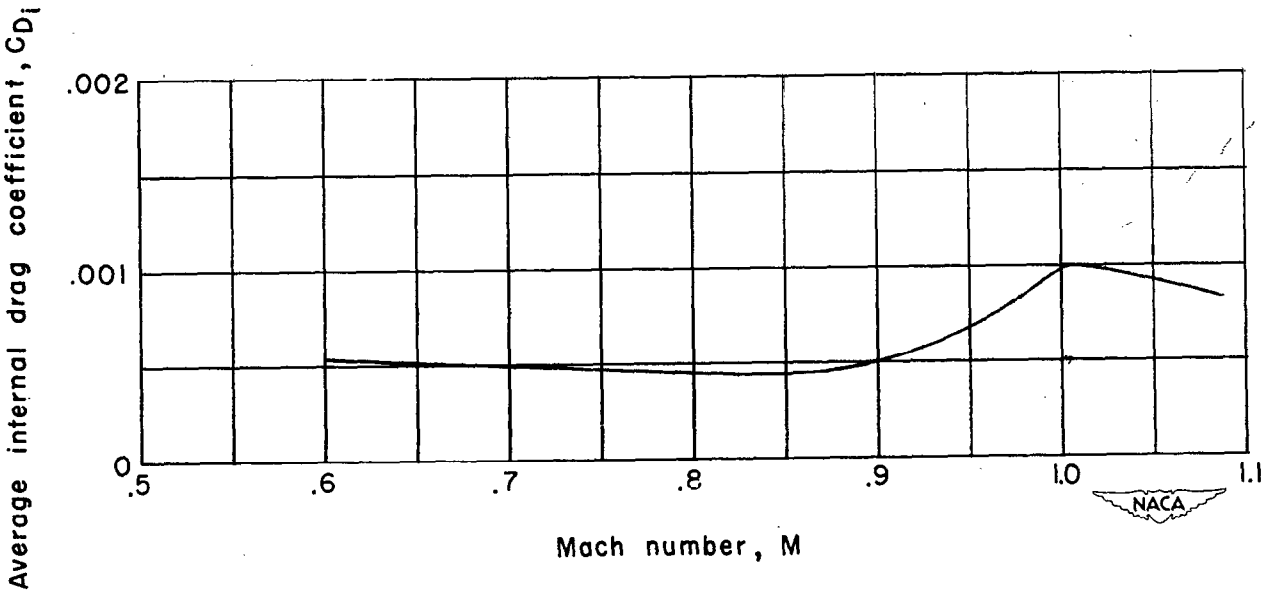

Figure 6.- Variation of average internal drag coefficient with Mach number.

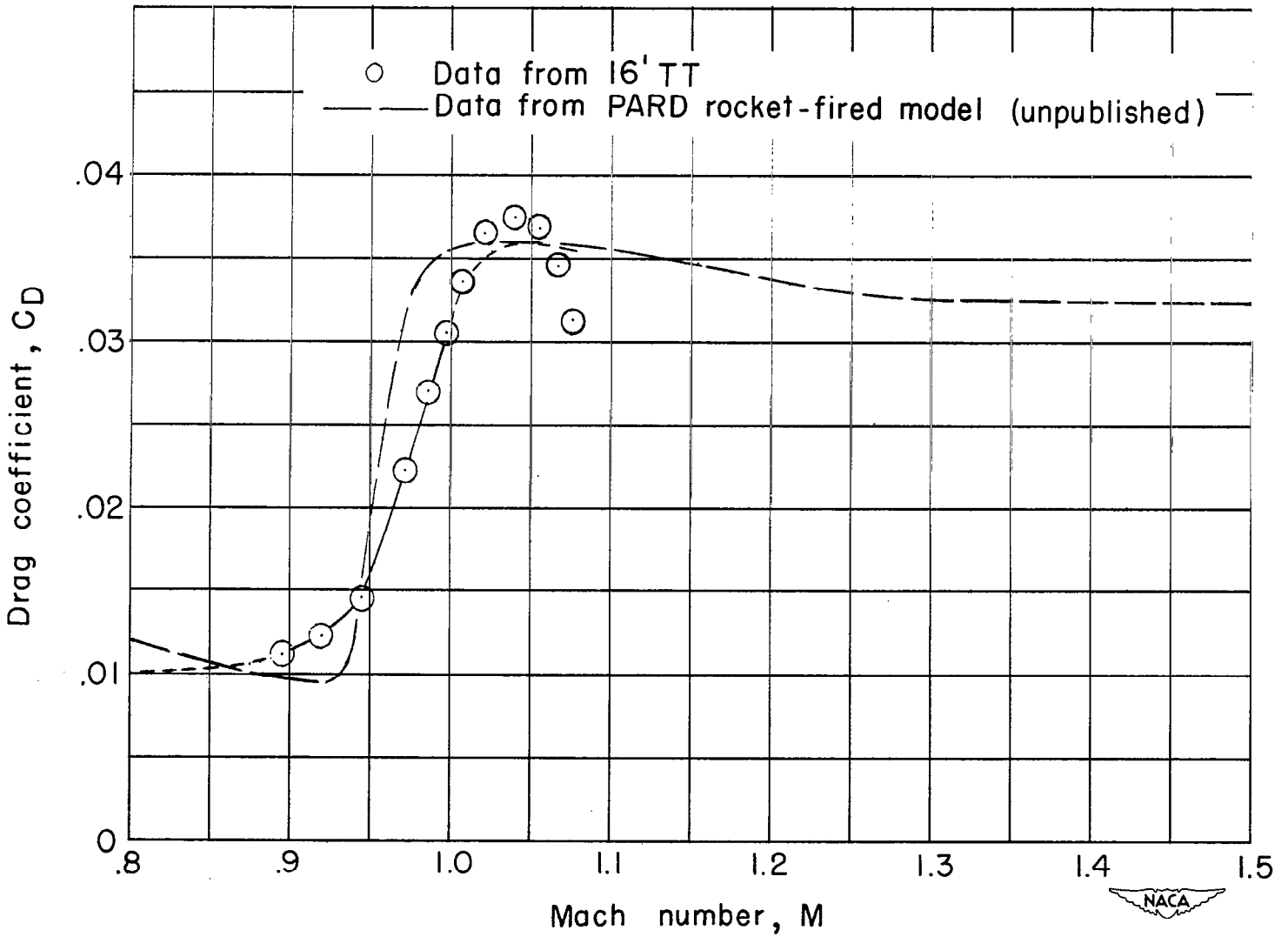

Figure 7.- Variation of drag coefficient with Mach number for the 1/10-scale model of the MX-1626 supersonic bomber.

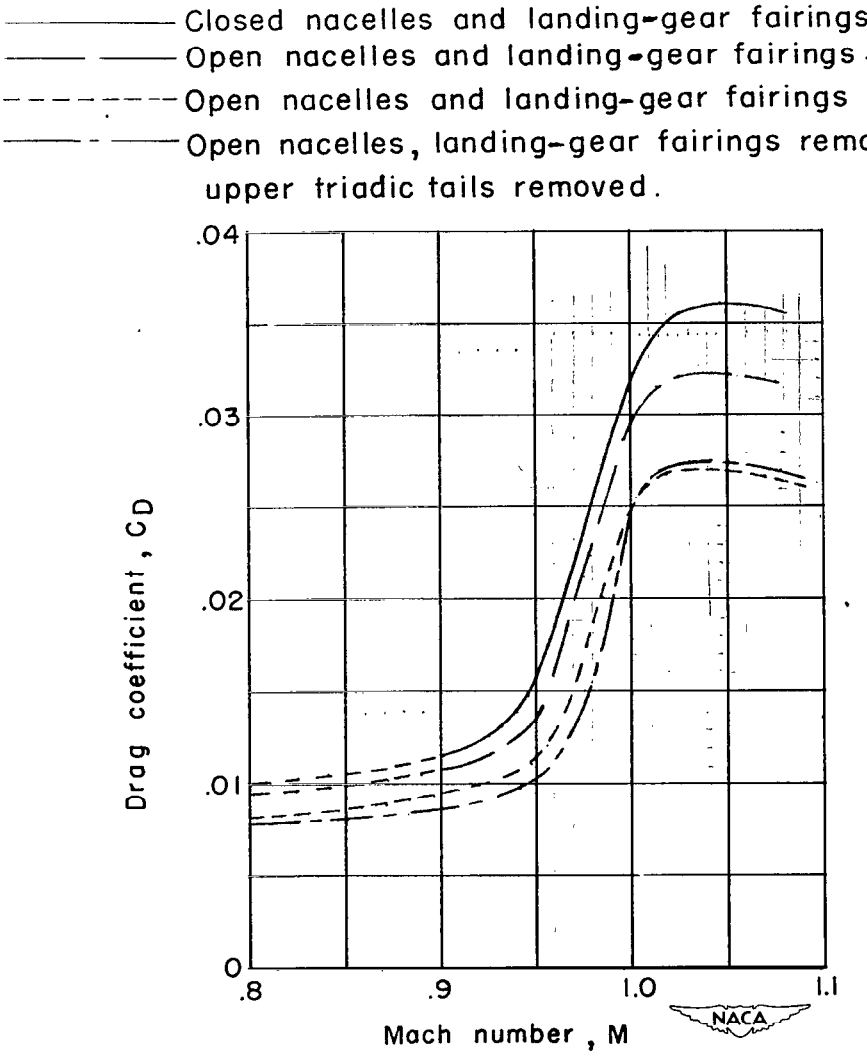

Figure 8.- Variation of drag coefficient with Mach number for various configurations of the 1/10-scale model of the MX-1626 supersonic bomber.

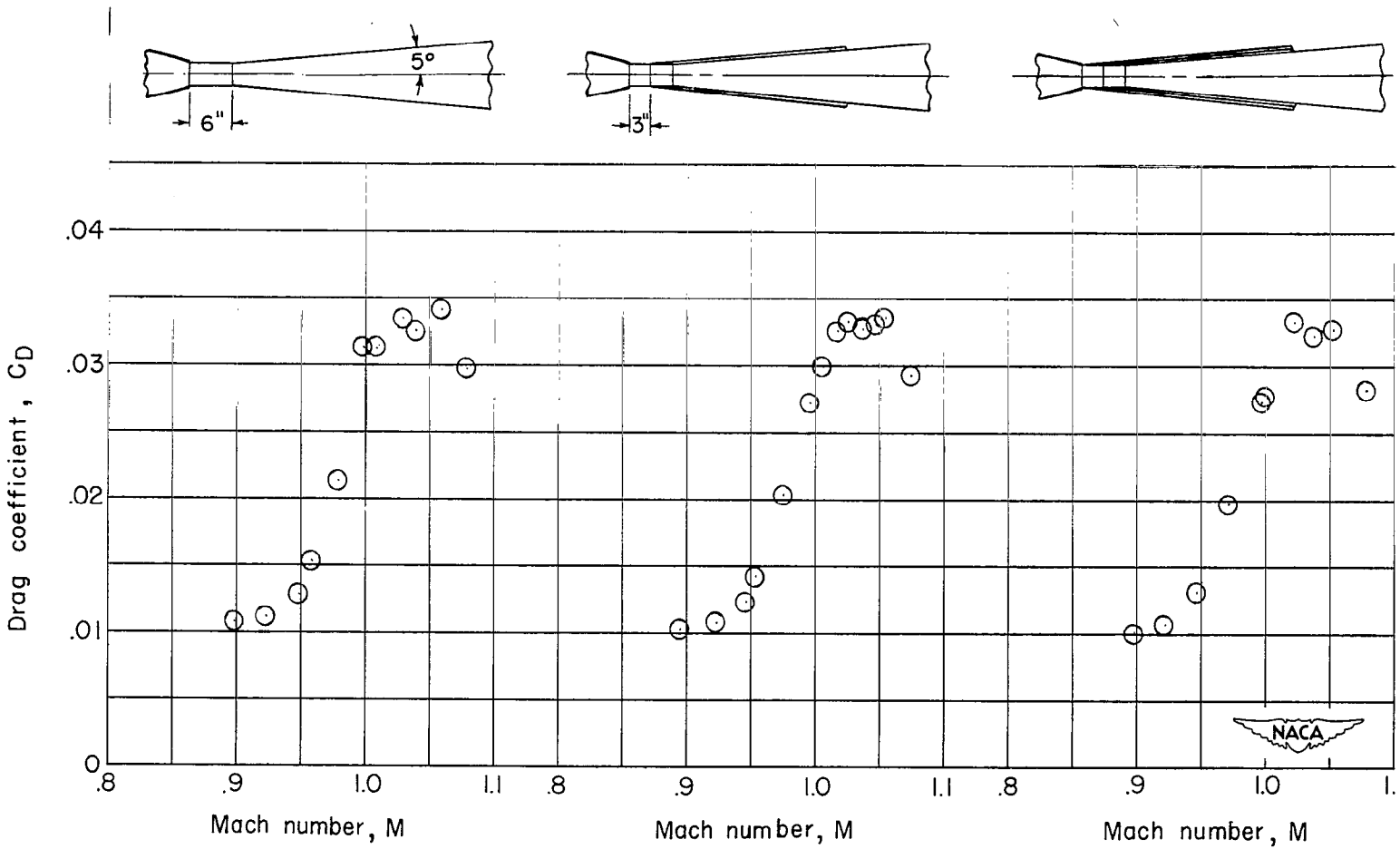

(a) No cuffs. (b) One cuff. (c) Two cuffs.

Figure 9.- Effect of sting cuffs on drag coefficient of 1/10-scale model of the MX-1626 supersonic bomber with open nacelles.

[redacted] UNCLASSIFIED

[redacted]